



## OPEN ACCESS

## EDITED BY

Andrea Bertoldi,  
ParisTech Institut d'Optique Graduate  
School, France

## REVIEWED BY

Lu Zhou,  
East China Normal University, China  
Jingjing Zheng,  
Beijing Jiaotong University, China

## \*CORRESPONDENCE

Wei Zhuang,  
✉ zhuangwei@nim.ac.cn  
Bin Luo,  
✉ luobin@bupt.edu.cn

## SPECIALTY SECTION

This article was submitted to Atomic and  
Molecular Physics,  
a section of the journal  
Frontiers in Physics

RECEIVED 05 November 2022

ACCEPTED 29 November 2022

PUBLISHED 09 December 2022

## CITATION

Guan X, Zhuang W, Shi T, Miao J,  
Zhang J, Chen J and Luo B (2022), Cold-  
atom optical filtering enhanced by  
optical pumping.  
*Front. Phys.* 10:1090483.  
doi: 10.3389/fphy.2022.1090483

## COPYRIGHT

© 2022 Guan, Zhuang, Shi, Miao, Zhang,  
Chen and Luo. This is an open-access  
article distributed under the terms of the  
[Creative Commons Attribution License  
\(CC BY\)](https://creativecommons.org/licenses/by/4.0/). The use, distribution or  
reproduction in other forums is  
permitted, provided the original  
author(s) and the copyright owner(s) are  
credited and that the original  
publication in this journal is cited, in  
accordance with accepted academic  
practice. No use, distribution or  
reproduction is permitted which does  
not comply with these terms.

# Cold-atom optical filtering enhanced by optical pumping

Xiaolei Guan<sup>1</sup>, Wei Zhuang<sup>2\*</sup>, Tiantian Shi<sup>3</sup>, Jianxiang Miao<sup>3</sup>,  
Jia Zhang<sup>3</sup>, Jingbiao Chen<sup>3,4</sup> and Bin Luo<sup>1\*</sup>

<sup>1</sup>State Key Laboratory of Information Photonics and Optical Communications, Beijing University of Posts and Telecommunications, Beijing, China, <sup>2</sup>National Institute of Metrology, Beijing, China, <sup>3</sup>State Key Laboratory of Advanced Optical Communication, Systems and Networks, School of Electronics, Peking University, Beijing, China, <sup>4</sup>Hefei National Laboratory, Hefei, China

Atomic optical filters such as Faraday anomalous dispersion optical filters (FADOFs) or similar technologies can achieve very narrow optical bandwidth close to the scale of atomic linewidth, which can be greatly reduced in cold atoms. However, limited by the number of cold atoms and the size of the cold atomic cloud, the number of atoms interacting with the laser is reduced, and the transmission remains as low as 2%. In this work, we introduce the optical pumping into the cold atomic optical filter to solve this problem. Circular polarized optical pumping can produce polarization of the atomic ensemble and induce dichromatic as well as the Faraday rotation. We demonstrate a cold-atom optical filter which operates on the  $^{87}\text{Rb } 5^2\text{S}_{1/2} (F=2)$  to  $5^2\text{P}_{3/2} (F'=2)$  transition at 780 nm. The filter achieves an ultranarrow bandwidth of 6.6(4) MHz, and its peak transmission is 15.6%, which is nearly 14 times higher than that of the cold-atom optical filter realized by Faraday magneto-optic effect. This scheme can be extended to almost all kinds of atomic optical filters and may find applications in self-stabilizing laser and active optical clock.

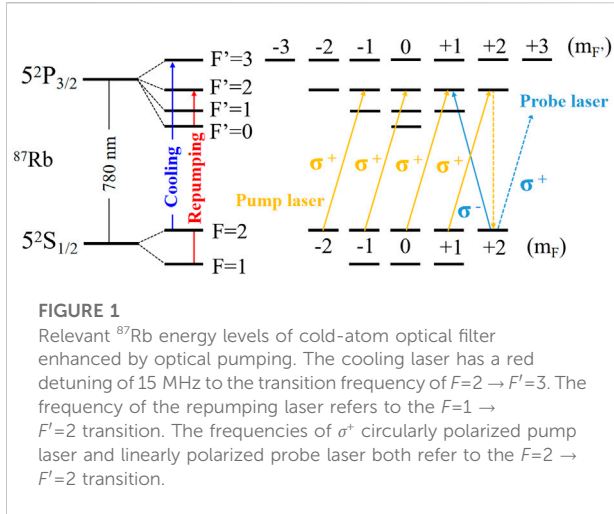
## KEYWORDS

optical filter, cold atom, optical pumping, induced circular dichroism, ultranarrow bandwidth

## 1 Introduction

Atomic optical filter is a device that uses the spectral characteristics of atomic resonance transition to achieve filtering function. It is mainly divided into two categories: Atomic resonance filter [1–4] (ARF) and optical rotation effect-based filter [5, 6] (such as Faraday anomalous dispersion optical filter [7, 8], FADOF). With the advantages of high peak transmission [9–12], narrow bandwidth [13–16], and excellent out-of-band suppression [17], the atomic optical filter can extract weak narrowband light signal from strong background light noise (including sunlight, scattered light, and artificial light, etc.). At present, it has played a key role in the fields of optical communication [18, 19], lidar [20, 21], and self-stabilizing laser [22, 23].

The induced-dichroism-excited atomic line filter [24] (IDEALF) is a novel rotation-based filter. Due to the reverse transmission of probe laser and pump laser, only atoms with very narrow velocity groups can be excited to participate in the filtering process, which effectively



reduces the influence of Doppler broadening on the filter. Therefore, many studies use this induced dichroism principle [25] to narrow the filter’s bandwidth. For example, these works, Refs. [26–30], on FADOF have improved the FADOF bandwidth from ~ 200 MHz down to ~ 20 MHz over the past two decades. However, it is still difficult to narrow the transmitted bandwidth of filters based on thermal atoms to the order of natural linewidth.

To overcome the Doppler effect caused by atomic motion and other factors related to atomic velocity in the process of interaction between light and atoms, the cold-atom FADOF has been studied [31]. By using laser cooling technology to slow down atoms, so as to reduce the influence of Doppler effect, they finally realized an ultranarrow-bandwidth cold-atom FADOF with bandwidth close to the natural linewidth of atomic transition. However, there is also a problem with the above research scheme, that is, the transmission is greatly sacrificed while the bandwidth of FADOF is narrowed. This is mainly because in the FADOF realized by thermal-atom scheme, the number of atoms in the vapor cell can reach  $10^{12}$ , while in the FADOF realized by cold-atom scheme, the number of cold atoms trapped by laser cooling technology is only about  $10^8$ . Although the density of the two gas atoms is approximately the same, the length of laser traveling in the cold atom medium is much shorter than that of the thermal atom. The decrease in the number of atoms interacting with the laser is detrimental to the atomic optical filter’s transmission. Therefore, how to improve the transmission as much as possible while ensuring the ultranarrow-bandwidth of FADOF is the key to current research.

## 2 Theory

In this study, the laser cooling technology is also used to narrow the atomic filter’s bandwidth, but it is combined with the optical pumping technology [32, 33]. Different from the previous

purpose of narrowing the transmitted bandwidth, we use the induced dichroism to improve the transmission of cold-atom optical filter. The relevant energy levels are shown in Figure 1.

When the  $\sigma^+$  circularly polarized pump laser is applied to the cold atoms, an asymmetric distribution of atoms will be constructed on the ground state magnetic sublevels. Thus, the left and right circularly polarized components of linearly polarized incident laser have different refractive indices. For thin atomic vapor, the refractive index of the incident laser can be expressed as [34]:

$$n(\delta) = 1 - \rho \frac{6\pi}{k^3} \frac{\delta/\Gamma}{1 + 4(\delta/\Gamma)^2} \tag{1}$$

Here,  $\rho$  is the density of gas atoms,  $k = \frac{2\pi}{\lambda}$  is the wave number in vacuum,  $\delta$  is the detuning between the incident laser and the central frequency of the atoms, and  $\Gamma$  is the natural linewidth of atomic transition. The polarization direction of linearly polarized probe laser will rotate after passing through the atomic medium. The rotation angle can be simply expressed as  $\phi = \pi(n_+ - n_-)L/\lambda$ , where  $L$  is the length of the atomic medium,  $\lambda$  is the probe laser wavelength,  $n_+$  and  $n_-$  are the refractive indices of  $\sigma^+$  and  $\sigma^-$  circularly polarized light components in linearly polarized probe laser.

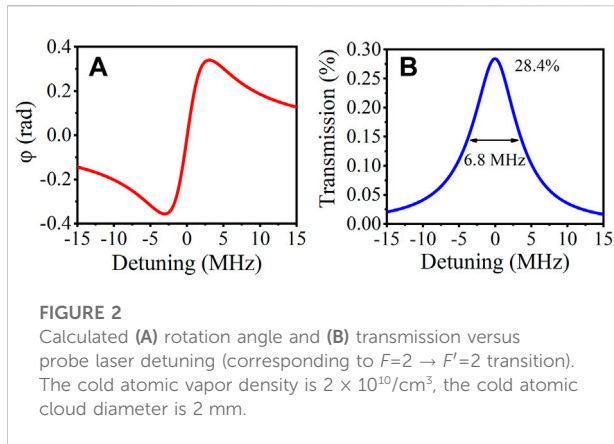
$$\sigma(\delta) = \frac{3\lambda^2}{2\pi} \frac{1}{1 + 4(\delta/\Gamma)^2} \tag{2}$$

The atoms also have absorption effect on incident laser. The effective atomic absorption cross-section can be defined as Eq. 2.  $\alpha(\delta) = \rho\sigma(\delta)$  is the absorption coefficient. Then, the transmission of the filter can be written as [8, 25]:

$$T = \frac{1}{2} \exp(-\bar{\alpha}L) [\cosh(\Delta\alpha L) - \cos(2\phi)] \tag{3}$$

where  $\bar{\alpha} = \frac{1}{2}(\alpha_+ + \alpha_-)$  is the mean absorption coefficient,  $\Delta\alpha = \frac{1}{2}(\alpha_+ - \alpha_-)$  is the circular dichroism,  $\alpha_+$  and  $\alpha_-$  are the absorption coefficients of  $\sigma^+$  and  $\sigma^-$  circularly polarized light components in linearly polarized probe laser. Due to the asymmetric population of atoms, only the  $\sigma^-$  circularly polarized light component in the linearly polarized probe laser can be absorbed, while the  $\sigma^+$  component is almost not (induced dichroism). The large difference in detuning ( $\delta$ ) between  $\sigma^+$  and  $\sigma^-$  results in the difference in refractive indices ( $n_+$  and  $n_-$ ) and absorption coefficients ( $\alpha_+$  and  $\alpha_-$ ), according to Eq. 1 and Eq. 2. Consequently, the rotation angle  $\phi$  and circular dichroism  $\Delta\alpha$  will increase, leading to an enhanced transmission, calculated from Eq. 3. Here, it is important to note that the maximum magnetic quantum number of the probe laser’s upper working energy level cannot be greater than that of the lower working energy level.

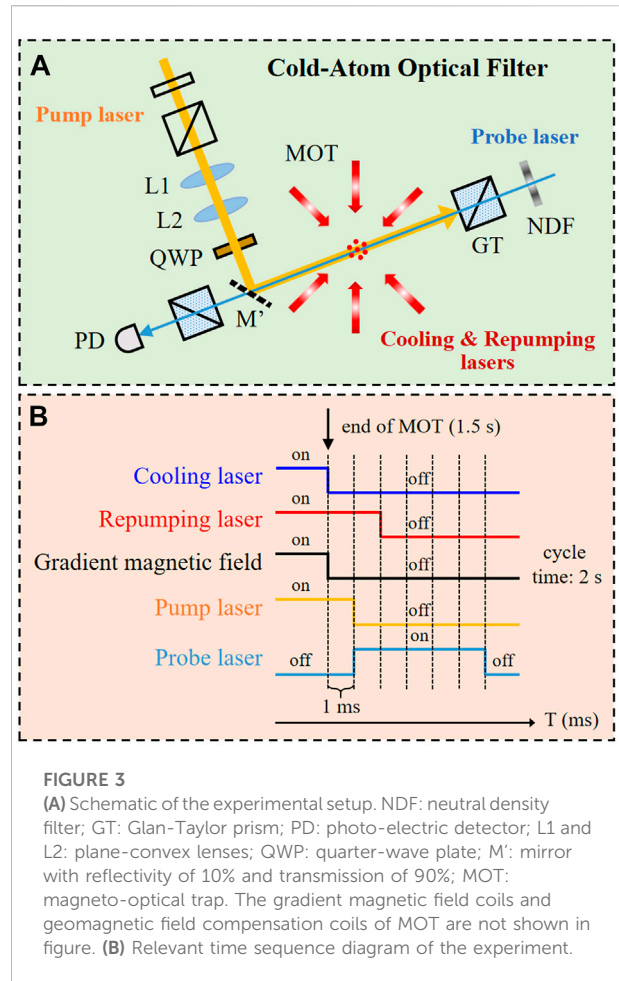
Corresponding to the actual working conditions of the experiment, when the cold atomic vapor density is  $2 \times 10^{10}/\text{cm}^3$  and the cold atomic cloud diameter is 2 mm, we obtain the



theoretical simulation results shown in Figure 2. The filter displays a single 6.8 MHz passband at a peak transmission of 28.4%. This bandwidth is slightly wider than the natural linewidth of atomic transition (6.1 MHz) because we take into account the effects of saturation broadening and residual Doppler broadening. Cold-atom optical filtering enhanced by optical pumping has another advantage, that is, its optical rotation is induced by optical pumping to bring an asymmetric population of atoms on the ground state Zeeman sublevels, rather than the sublevel splitting by a magnetic field. Therefore, it does not need an additional uniform magnetic field, which is a technical innovation different from the previous cold-atom FADOF.

### 3 Experimental setup and methods

The scheme of the experimental setup is presented in Figure 3. The first step of our study is to prepare cold  $^{87}\text{Rb}$  atoms by magneto-optical trap (MOT). We lock the cooling laser and repumping laser to  $F=2 \rightarrow F'=3$  and  $F=1 \rightarrow F'=1$  transitions using the standard saturated absorption spectroscopy technique. Then, we red-detune the former by 15 MHz for cooling and blue-detune the latter towards  $F'=2$  for repumping. After frequency stabilization, the cooling and repumping lasers are combined and then divided into six beams with the same power, which are injected into the optical windows of the vacuum system in pairs (The power of each cooling laser is about 6 mW, and each repumping laser is about 1.5 mW, the diameter of each laser beam is about 10 mm). The vacuum system (vacuum level:  $2 \times 10^{-9}$  Torr) contains thin  $^{87}\text{Rb}$  atomic vapor. The gradient magnetic field of MOT is provided by a pair of coils with current in opposite directions. Finally, we trap around  $2 \times 10^8$  atoms in the MOT with a temperature of around 200  $\mu\text{K}$ . The diameter of the cold atomic cloud is about 2 mm, the density of the cold atomic vapor is about  $10^{10}/\text{cm}^3$ .



Next, we carry out the construction of cold-atom optical filter and its pump light path and probe light path. Using the modulation transfer spectrum (MTS) frequency stabilization technology, the 780 nm probe laser is locked to the  $F=2 \rightarrow F'=3$  transition, and then red-shifted 267 MHz to  $F'=2$  by an acousto-optic modulator (AOM). After frequency stabilization, the probe laser is firstly transmitted to the neutral density filter (NDF) to adjust the laser power. Then, it passes through the cold atomic cloud trapped in the vacuum system, a pair of Glan-Taylor prisms (GTPs) with orthogonal polarization direction, and then enters the photo-electric detector (PD), which measures the transmitted signal of the cold-atom optical filter. On the other side, a beam is divided from the 780 nm cooling laser, it is used as the pump laser for this study, and its frequency is adjusted to the  $F=2 \rightarrow F'=2$  transition by an AOM. This pump laser passes through a half-wave plate (HWP), a polarizing beam splitter (PBS), a pair of plane-convex lenses (L1 and L2), and a quarter-wave plate (QWP), then reflected by a mirror with reflectivity of 10% and transmission of 90% (M'). The reflected pump laser overlaps with the probe laser in reverse and passes through

**TABLE 1** Power, Beam diameter, and polarization of the Cooling, Repumping, Pump, and Probe lasers.

	Power	Beam diameter (mm)	Polarization
Cooling laser	6 mW/beam	10	$\sigma^+$ and $\sigma^-$
Repumping laser	1.5 mW/beam	10	$\sigma^+$ and $\sigma^-$
Pump laser	1.5 mW	8	$\sigma^+$
Probe laser	3 $\mu$ W	1	linearly polarized

the cold atomic cloud trapped in the vacuum system. Here, HWP and PBS are used to adjust the pump laser power and turn the pump laser into a pure linearly polarized light. L1 and L2 are used to expand the pump laser beam, letting the pump laser completely contains cold atomic cloud when passing through the vacuum system, so as to improve the efficiency of optical pumping. QWP is used to convert the linearly polarized pump laser into a standard  $\sigma^+$  circularly polarized pump laser.

## 4 Results and analysis

Setting 2 s as a cycle, the MOT (cooling laser and gradient magnetic field) is switched off at 1.5 s. Then, after a time interval of 1 ms, turn off the pump laser and immediately turn on the probe laser to measure the transmitted signal of the cold-atom optical filter. The repumping laser is kept on during the whole cooling and pumping process, in order to return the atoms from  $F=1$  to  $F=2$ . The AOM placed on the probe light path can be used for fast switching the probe laser. Under the experimental conditions shown in Table 1, we use the above AOM to generate frequency detuning near the probe laser resonance frequency, discretely measure the transmission values at multiple frequency points, and then draw

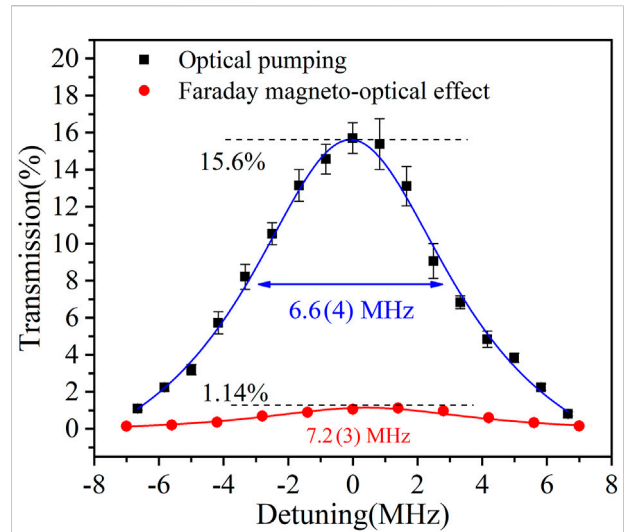


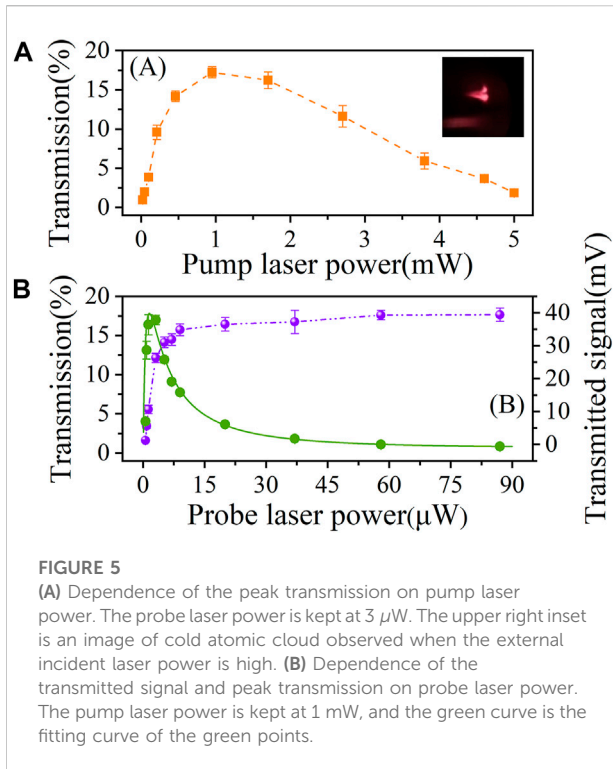
**FIGURE 4** Transmission spectrum of the cold-atom optical filter (corresponding to  $F=2 \rightarrow F'=2$  transition). The black square points represent the transmission spectrum of the cold-atom optical filter realized by optical pumping method. The red circular points represent the transmission spectrum of the cold-atom optical filter realized by Faraday magneto-optical effect. The blue and red curves are the Lorentz fitting curves respectively. Each point is obtained by averaging 20 measurements.

them in combination. Thus, the transmission spectrum of the cold-atom optical filter which operates on the  $F=2 \rightarrow F'=2$  transition is obtained (see the black square points in Figure 4). Using Lorentz fitting (blue curve), it can be concluded that the transmitted bandwidth of the cold-atom optical filter realized by optical pumping method is 6.6(4) MHz, and the peak transmission is 15.6%.

We also measure the transmission spectrum of the cold-atom optical filter realized by Faraday magneto-optical effect under the same transition. The pump laser is blocked during the whole process. The homogeneous magnetic field (around 4 Gs) along the probe laser direction is generated by a pair of energized coils.

**TABLE 2** Peak transmission, ENBW, and FOM parameters for different filters.

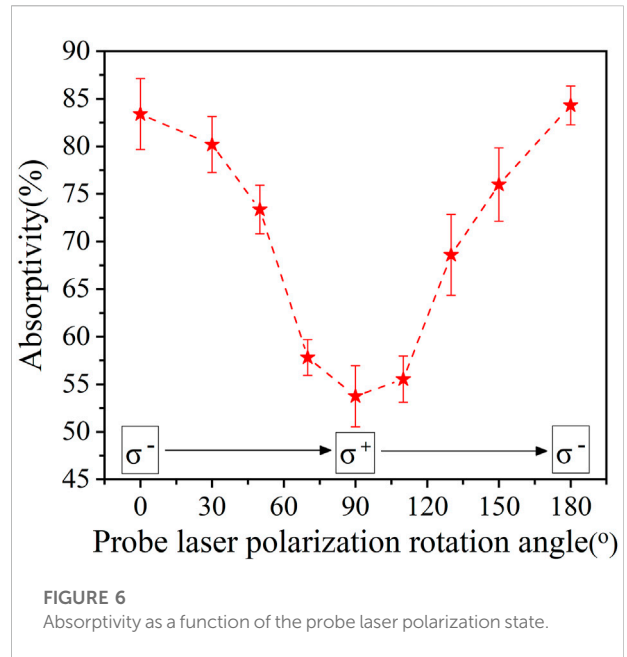
Element	Line	Peak transmission (%)	ENBW	FOM ( $\text{GHz}^{-1}$ )	References
Na	D2	90.69	6.95 GHz	0.13	[36]
Na	D2	86.17	5.05 GHz	0.17	[38]
K	D1	94.92	3.22 GHz	0.29	[39]
Cs	D2	78.69	1.55 GHz	0.51	[16]
Cs	D1	76.77	0.96 GHz	0.8	[16]
$^{85}\text{Rb}$	D1	55.63	3.92 GHz	0.14	[40]
Rb	D2	89.30	2.53 GHz	0.35	[17]
Rb	D2	68.46	0.42 GHz	1.63	[37]
$^{87}\text{Rb}$	D2	15.60	6.6(4) MHz	23.6	This work



We still keep the MOT off at 1.5 s, then turn on the probe laser and homogeneous magnetic field at 1.501 s to measure the cold-atom FADOF's transmitted signal. According to the same data recording and processing method, we get the transmission spectrum, seeing the red circular points in Figure 4, the red curve is its Lorentz fitting curve. From the comparison, it can be clearly seen that the cold-atom optical filters implemented by the two different schemes all have an ultranarrow bandwidth close to the natural linewidth of atomic transition. However, the peak transmission of the cold-atom optical filter realized by optical pumping method (15.6%) is nearly 14 times higher than that of the cold-atom optical filter realized by Faraday magneto-optical effect (1.14%), which is a significant progress made in this study.

Apart from narrow bandwidth and high peak transmission, figure of merit [35, 36] (FOM) is another important quality measure for the filter, defined as  $FOM = T_{\max}/ENBW$ .  $T_{\max}$  is the maximum transmission of the filter,  $ENBW = \int T(\nu)d\nu/T_{\max}$  is the equivalent noise bandwidth, and  $\nu$  is the optical frequency. After calculation, the cold-atom optical filter realized by optical pumping method in this study has a FOM value of  $23.6 \text{ GHz}^{-1}$ , which is 14 times larger than the largest FOM achieved by thermal vapor atomic optical filter published to date [37]. Here, we list the peak transmission, ENBW, and FOM parameters for a variety of filters given in the literature, as shown in Table 2.

To investigate the influence of pump laser power on the peak transmission of cold-atom optical filter, we vary its power under the probe laser power kept at  $3 \mu\text{W}$ . From Figure 5A, it can be seen that



the transmission increases with the pump laser power and reaches the maximum when the pump laser power is 1 mW. After that, continue to increase the pump laser power, due to the pump laser exerts a greater force on the cold atoms, resulting in the diffusion and displacement of cold atomic cloud (see the upper right inset in Figure 5A), the transmission of the cold-atom optical filter decreases rapidly. Figure 5B shows that when the pump laser power is 1 mW, the intensity of the transmitted signal gradually becomes saturated with the increase of the probe laser power. Since the intensity of the incident laser increases linearly with the probe laser power, the measured transmission points show a trend of first increasing and then decreasing [31, 41]. From the green fitting curve, we can conclude that when the probe laser power is about  $2 \mu\text{W}$ , the transmission of the filter reaches a maximum.

Finally, we use a simple and direct method to verify the effect of optical pumping. Before the probe laser enters the cold-atom optical filter, let it pass through a quarter-wave plate, which can convert the linearly polarized probe laser into circularly polarized. Then, removing the two GTPs and using the PD to receive the absorption signal of trapped cold atoms. In combination with the energy levels shown in Figure 1, rotating the above quarter-wave plate, when the probe laser is  $\sigma^-$  circularly polarized, it can be absorbed by the atoms located on the ground state  $F=2$ ,  $m_F = +2$  level, making the atoms transition to the excited state  $F=2$ ,  $m_F = +1$ . However, when the probe laser is  $\sigma^+$  circularly polarized, because there is no excited state energy level can transition, the absorption of light by cold atoms will be greatly reduced.

Under different polarization states of the probe laser, the absorptivity change actually measured in this study is shown in Figure 6, which is indeed consistent with the above analysis. As the probe laser polarization changes from  $\sigma^-$  to  $\sigma^+$ , the

absorptivity decreases gradually, and *vice versa*. If the optical pumping does not work or the effect is not obvious, the atoms will be evenly distributed on all the sublevels of the ground state  $F=2$ , then there will be no significant difference in absorptivity. In addition, it should be noted that when the probe laser polarization is  $\sigma^+$ , the absorptivity is still 50% instead of 0. This may be because the optical pumping does not accumulate all the atoms to  $F=2$ ,  $m_F = +2$  level, and there are still a small number of atoms distributed in other Zeeman sublevels, which results in the absorption of  $\sigma^+$  circularly polarized probe laser. And this is also the reason for the deviation between the theoretical simulation “transmission” and the experimental measurement “transmission”. But in any case, this study achieves a good optical pumping effect, which also greatly improves the transmission of the cold-atom optical filter.

## 5 Conclusion

In conclusion, using laser cooling and optical pumping technologies, we demonstrate a cold-atom optical filter which operates on the  $^{87}\text{Rb } F=2 \rightarrow F'=2$  transition at 780 nm, with an ultranarrow bandwidth of 6.6(4) MHz and a peak transmission of 15.6%. The scheme we proposed effectively solves the problem of the decrease of filter transmission due to the loss of atom number. Experimental results show that, under the same transition, the peak transmission of our achieved cold-atom optical filter (15.6%) is nearly 14 times higher than that of the cold-atom optical filter realized by Faraday magneto-optic effect (1.14%).

We can further improve the transmission of cold-atom optical filter by increasing the optical thickness (OD), which is specifically influenced by the density of gas atoms and the length of atomic medium [42]. An ultranarrow-bandwidth filter with high transmission might reveal active optical frequency standard [43] without an additional locked pump laser. In this case, the pump laser will not disturb the center frequency of the output laser, which is determined by the atomic transmission. Furthermore, trapping atoms in MOT on chip [44, 45] can expand optical frequency standard's applications in the future, for its less cost and complexity. And the problem of cold-atom filter operating in pulse mode may be solved by using optical molasses to prepare cold atoms. Finally, a cold-atom optical filter using narrower natural linewidth has the potential to be applied in more ultranarrow-bandwidth-required fields.

## Data availability statement

The original contributions presented in the study are included in the article/supplementary material, further inquiries can be directed to the corresponding authors.

## Author contributions

BL, WZ, and JC conceived the idea of the cold-atom optical filtering enhanced by optical pumping. XG performed the experiments and carried out the theoretical calculations. XG wrote the manuscript. TS, JM, and JZ provided revisions. All authors contributed equally to the discussions of the results.

## Funding

This research was funded by the National Natural Science Foundation of China (61771067, 11704361); Innovation Program for Quantum Science and Technology (2021ZD0303200); Wenzhou Key Scientific and Technological Innovation R&D Project (Application No. 2019ZG0029); Wenzhou Major Science & Technology Innovation Key Project (Grant No. ZG2020046); China Postdoctoral Science Foundation (BX2021020).

## Acknowledgments

We give our best wishes on the occasion of Yiqiu Wang's 90th birthday. The authors have learned a lot from Wang throughout their 10 years of collaboration and communication. For their research on cold atoms and optical filter, authors most frequently refer to Wang's book *Laser Cooling and Trapping of Atoms*, and *Principle of Quantum Frequency Standard*. Wang's rigorous academic attitude and profound professional knowledge are worth learning from each of us. We sincerely wish Wang to be healthy and happy.

## Conflict of interest

The authors declare that the research was conducted in the absence of any commercial or financial relationships that could be construed as a potential conflict of interest.

## Publisher's note

All claims expressed in this article are solely those of the authors and do not necessarily represent those of their affiliated organizations, or those of the publisher, the editors and the reviewers. Any product that may be evaluated in this article, or claim that may be made by its manufacturer, is not guaranteed or endorsed by the publisher.

## References

- Marling JB, Nilsen J, West LC, Wood LL. An ultrahigh-Q isotropically sensitive optical filter employing atomic resonance transitions. *J Appl Phys* (1979) 50(2): 610–4. doi:10.1063/1.326074
- Shay TM, Chung YC. Ultrahigh-resolution, wide-field-of-view optical filter for the detection of frequency-doubled Nd:YAG radiation. *Opt Lett* (1988) 13(6):443–5. doi:10.1364/ol.13.000443
- Gelbwachs JA. Atomic resonance filters. *IEEE J Quan Electron* (1988) 24(7): 1266–77. doi:10.1109/3.963
- Gelbwachs JA. Active wavelength-shifting in atomic resonance filters. *IEEE J Quan Electron* (1990) 26(6):1140–7. doi:10.1109/3.108112
- Menders J, Searcy P, Roff K, Korevaar E. Blue cesium Faraday and Voigt magneto-optic atomic line filters. *Opt Lett* (1992) 17(19):1388–90. doi:10.1364/ol.17.001388
- Billmers RI, Gayen SK, Squicciarini MF, Contarino VM, Scharpf WJ. Experimental demonstration of an excited-state Faraday filter operating at 532 nm. *Opt Lett* (1995) 20(1):106–8. doi:10.1364/ol.20.000106
- Ohman Y. On some new auxiliary instruments in astrophysical research VI. A tentative monochromator for solar work based on the principle of selective magnetic rotation. *Stockholms Obs Ann* (1956) 19(4):9–11.
- Yeh P. Dispersive magneto-optic filters. *Appl Opt* (1982) 21(11):2069–75. doi:10.1364/ao.21.002069
- Yin B, Shay TM. Faraday anomalous dispersion optical filter for the Cs 455 nm transition. *IEEE Photon Technol Lett* (1992) 4(5):488–90. doi:10.1109/68.136496
- Wang Y, Zhang X, Wang D, Tao Z, Zhuang W, Chen J. Cs Faraday optical filter with a single transmission peak resonant with the atomic transition at 455 nm. *Opt Express* (2012) 20(23):25817–25. doi:10.1364/oe.20.025817
- Ling L, Bi G. Isotope  $^{87}\text{Rb}$  Faraday anomalous dispersion optical filter at 420 nm. *Opt Lett* (2014) 39(11):3324–7. doi:10.1364/ol.39.003324
- Xue X, Pan D, Zhang X, Luo B, Chen J, Guo H. Faraday anomalous dispersion optical filter at  $^{133}\text{Cs}$  weak 459 nm transition. *Photon Res* (2015) 3(5):275–8. doi:10.1364/prj.3.000275
- BloomLiuMenders SHCSJ, Benson K, Korevaar E. Ultranarrow line filtering using a Cs Faraday filter at 852 nm. *Opt Lett* (1991) 16(11):846–8. doi:10.1364/ol.16.000846
- Zielińska JA, Beduini FA, Godbout N, Mitchell MW. Ultranarrow Faraday rotation filter at the Rb  $D_1$  line. *Opt Lett* (2012) 37(4):524–6. doi:10.1364/ol.37.000524
- Wang Y, Zhang S, Wang D, Tao Z, Hong Y, Chen J. Nonlinear optical filter with ultranarrow bandwidth approaching the natural linewidth. *Opt Lett* (2012) 37(19):4059–61. doi:10.1364/ol.37.004059
- Zentile MA, Whiting DJ, Keaveney J, Adams CS, Hughes IG. Atomic Faraday filter with equivalent noise bandwidth less than 1 GHz. *Opt Lett* (2015) 40(9):2000. doi:10.1364/ol.40.002000
- Dick DJ, Shay TM. Ultrahigh-noise rejection optical filter. *Opt Lett* (1991) 16(11):867–9. doi:10.1364/ol.16.000867
- Tang J, Wang Q, Li Y, Zhang L, Gan J, Duan M, et al. Experimental study of a model digital space optical communication system with new quantum devices. *Appl Opt* (1995) 34(15):2619–22. doi:10.1364/ao.34.002619
- Zhang J, Gao G, Wang B, Guan X, Yin L, Chen J, et al. Background noise resistant underwater wireless optical communication using Faraday atomic line laser and filter. *J Lightwave Technol* (2022) 40(1):63–73. doi:10.1109/jlt.2021.3118447
- Popescu A, Walther T. On an ESFADOF edge-filter for a range resolved Brillouin-lidar: The high vapor density and high pump intensity regime. *Appl Phys B* (2010) 98(4):667–75. doi:10.1007/s00340-009-3857-5
- Yang Y, Cheng X, Li F, Hu X, Lin X, Gong S. A flat spectral Faraday filter for sodium lidar. *Opt Lett* (2011) 36(7):1302–4. doi:10.1364/ol.36.001302
- Wanninger P, Valdez EC. Diode-laser frequency stabilization based on the resonant Faraday effect. *IEEE Photon Technol Lett* (1992) 4(1):94–6. doi:10.1109/68.124888
- Tao Z, Hong Y, Luo B, Chen J, Guo H. Diode laser operating on an atomic transition limited by an isotope  $^{87}\text{Rb}$  Faraday filter at 780 nm. *Opt Lett* (2015) 40(18):4348–51. doi:10.1364/ol.40.004348
- Gayen SK, Billmers RI, Contarino VM, Squicciarini MF, Scharpf WJ, Yang G, et al. Induced-dichroism-excited atomic line filter at 532 nm. *Opt Lett* (1995) 20(12):1427–9. doi:10.1364/ol.20.001427
- He Z, Zhang Y, Wu H, Yuan P, Liu S. Theoretical model for an atomic optical filter based on optical anisotropy. *J Opt Soc Am B* (2009) 26(9):1755–9. doi:10.1364/josab.26.001755
- Turner LD, Karaganov V, Teubner PJO, Scholten RE. Sub-Doppler bandwidth atomic optical filter. *Opt Lett* (2002) 27(7):500–2. doi:10.1364/ol.27.000500
- Cerè A, Parigi V, Abad M, Wolfgramm F, Predojević A, Mitchell MW. Narrowband tunable filter based on velocity-selective optical pumping in an atomic vapor. *Opt Lett* (2009) 34(7):1012–4. doi:10.1364/ol.34.001012
- Liu S, Zhang Y, Wu H, Yuan P. Ultra-narrow bandwidth atomic filter based on optical-pumping-induced dichroism realized by selectively saturated absorption. *Opt Commun* (2012) 285(6):1181–4. doi:10.1016/j.optcom.2011.10.042
- Zhang X, Tao Z, Zhu C, Hong Y, Zhuang W, Chen J. An all-optical locking of a semiconductor laser to the atomic resonance line with 1 MHz accuracy. *Opt Express* (2013) 21(23):28010–8. doi:10.1364/oe.21.028010
- Zhuang W, Hong Y, Gao Z, Zhu C, Chen J. Ultranarrow bandwidth nonlinear Faraday optical filter at rubidium  $D_2$  transition. *Chin Opt Lett* (2014) 12(10): 101204. doi:10.3788/col201412.101204
- Zhuang W, Zhao Y, Wang S, Fang Z, Fang F, Li T. Ultranarrow bandwidth Faraday atomic filter approaching natural linewidth based on cold atoms. *Chin Opt Lett* (2021) 19(3):030201. doi:10.3788/col202119.030201
- Liu S, Zhang Y, Wu H, Yuan P. Atomic filter with large scale tunability. *J Opt Soc Am B* (2011) 28(5):1100–3. doi:10.1364/josab.28.001100
- Luo B, Yin L, Xiong J, Chen J, Guo H. Induced-Dichroism-Excited atomic line filter at 1529 nm. *IEEE Photon Technol Lett* (2018) 30(17):1551–4. doi:10.1109/lpt.2018.2860947
- Labeyrie G, Miniatura C, Kaiser R. Large Faraday rotation of resonant light in a cold atomic cloud. *Phys Rev A (Coll Park)* (2001) 64(3):033402. doi:10.1103/physreva.64.033402
- Zentile MA, Keaveney J, Mathew RS, Whiting DJ, Adams CS, Hughes IG. Optimization of atomic Faraday filters in the presence of homogeneous line broadening. *J Phys B: Mol Opt Phys* (2015) 48(18):185001. doi:10.1088/0953-4075/48/18/185001
- Kiefer W, Löw R, Wrachtrup J, Gerhardt I. Na-Faraday rotation filtering: The optimal point. *Sci Rep* (2014) 4(1):6552. doi:10.1038/srep06552
- Logue FD, Briscoe JD, Pizzey D, Wrathmall SA, Hughes IG. Better magneto-optical filters with cascaded vapor cells. *Opt Lett* (2022) 47(12):2975–8. doi:10.1364/ol.459291
- Hu Z, Sun X, Liu Y, Fu L, Zeng X. Temperature properties of Na dispersive Faraday optical filter at  $D_1$  and  $D_2$  line. *Opt Commun* (1998) 156(4-6):289–93. doi:10.1016/s0030-4018(98)00461-1
- Zhang Y, Jia X, Ma Z, Wang Q. Potassium Faraday optical filter in line-center operation. *Opt Commun* (2001) 194(1-3):147–50. doi:10.1016/s0030-4018(01)01222-6
- Luo B, Yin L, Xiong J, Chen J, Guo H. Signal intensity influences on the atomic Faraday filter. *Opt Lett* (2018) 43(11):2458–61. doi:10.1364/ol.43.002458
- Zheng B, Cheng H, Meng Y, Xiao L, Wan J, Liu L. Observation of Faraday rotation in cold atoms in an integrating sphere. *Chin Phys Lett* (2014) 31(7):073701. doi:10.1088/0256-307x/31/7/073701
- Wan J, Wang X, Zhang X, Meng Y, Wang W, Sun Y, et al. Quasi-one-dimensional diffuse laser cooling of atoms. *Phys Rev A (Coll Park)* (2022) 105(3): 033110. doi:10.1103/physreva.105.033110
- Zhuang W, Chen J. Active Faraday optical frequency standard. *Opt Lett* (2014) 39(21):6339–42. doi:10.1364/ol.39.006339
- Nshii CC, Vangeleyn M, Cotter JP, Griffin PF, Hinds EA, Ironside CN, et al. A surface-patterned chip as a strong source of ultracold atoms for quantum technologies. *Nat Nanotechnol* (2013) 8(5):321–4. doi:10.1038/nnano.2013.47
- Chen L, Huang C, Xu X, Zhang Y, Ma D, Lu Z, et al. Planar-Integrated magneto-optical trap. *Phys Rev Appl* (2022) 17(3):034031. doi:10.1103/physrevapplied.17.034031